Proceedings World Geothermal Congress 2020+1
Reykjavik, Iceland, April - October 2021

Suitability of the Aquistore CCS site for a CO_2 Circulation Test: Towards CO_2-Plume Geothermal (CPG) Power Plant Implementations

Kevin P. Hau[1], Alireza Rangriz-Shokri[2], Erik Nickel[3], Rick J. Chalaturnyk[2], Martin O. Saar[1,4]

[1]Geothermal Energy & Geofluids Group, Institute of Geophysics, Department of Earth Sciences, ETH Zurich, Zurich, Switzerland, (hauk@ethz.ch; saarm@ethz.ch)

[2]Department of Civil and Environmental Engineering, University of Alberta, Edmonton, AB, Canada

[3]Petroleum Technology Research Centre, Regina, SK, Canada

[4]Department of Earth and Environmental Sciences, University of Minnesota, Minneapolis, MN, USA

Keywords: CO_2 Plume Geothermal; CO_2 Circulation; CO_2 Storage; CCUS; Aquistore; Numerical Simulation; TRL

ABSTRACT

It is commonly accepted that a drastic decrease in global carbon dioxide (CO_2) emissions is necessary in order to reach the climate goals set by the Paris agreement in 2015. A key technology towards achieving that goal is CCUS - Carbon, Capture, Utilisation, and Sequestration. By using supercritical CO_2 instead of brine/water as a geothermal working fluid, geothermal energy production can possibly be expanded to regions with lower temperature gradients in subsurface formations, while permanently storing the CO_2 underground.

This first-order, conceptual study investigates the suitability of the Aquistore CCS site for a CO_2 circulation pilot test. For doing so, numerical simulations were performed to learn about the site responses to CO_2-circulation, the amount of back-produced CO_2 versus brine, and to estimate the flow behaviour in a potential CO_2 gas production well. A key requirement for a successful CO_2 circulation pilot test is to prevent liquid loading in the CO_2 gas production well. Liquid loading occurs when a liquid (here brine or water) accumulates in the production well. It can be avoided by maintaining an annular flow regime in the multi-phase fluid production stream in the production well. The resulting flow regime is mainly controlled by the total fluid mass flow rate in the production well. The flow regime in the production well also depends strongly on the overall transmissivity of the reservoir.

Our simulation results suggest that steady-state conditions will likely occur within weeks to a few months after the start of CO_2 circulation. Moreover, our results show that the amount of back-produced CO_2 is one order of magnitude larger than the amount of back-produced brine. In the majority of cases, we observe that the back-produced fluid production stream will ultimately flow in an annular flow pattern. Further analyses of CO_2 circulation results indicate a need for better characterisations of the subsurface multiphase fluid flow behaviour. To this end, we discuss attempts to constrain the uncertainty associated with the Aquistore reservoir characterisation and CO_2 plume growth through high-resolution history matching of non-isothermal injection data and time-lapse seismic monitoring surveys.

1. INTRODUCTION

Carbon capture and storage (CCS) will play a major role in addressing the global climate crisis (Global CCS Institute, 2020). As of now, one of the main reasons preventing the large-scale realisation of CCS are financial reasons (Randolph and Saar, 2011a,b). CO_2 plume geothermal systems (CPG) have the potential to strongly decrease the costs of traditional CCS sites by utilising geothermal energy from the subsurface (e.g. Randolph and Saar, 2011a,b; Adams et al., 2015; Garapati et al., 2015; Adams et al., 2020). In order to improve the technology readiness level (TRL) of CPG systems, it is essential to carry out a field-scale CPG pilot test. Note that a first successful CPG pilot test does not necessarily need to demonstrate that geothermal energy can be utilised to generate power. Instead, such a test should mainly show that stable CO_2 circulation between an injector and a producer within the CO_2 plume can be achieved and maintained. Thus, this type of a CPG pilot test is better referred to as a CO_2 circulation test.

Our first-order conceptual study investigates the feasibility of a CO_2 circulation test at the Aquistore project in Canada. Aquistore is a subsurface CO_2 storage complex associated with a post-combustion CO_2 capture plant at the Boundary Dam coal-fired power plant facility. Located near Estevan, Saskatchewan, in the central plains of Canada, Aquistore has, as of this writing, stored over 330 ktonnes of CO_2 underground. The storage complex consists of two wells, an injector and a monitoring well, spaced 151 m apart, drilled to depths of approximately 3400 m. The injector well is fitted with tubing, with a packer set at 3042 m (Rostron et al., 2014), and the casing is perforated in the porous intervals below the packer. The monitoring well is simply cased and has no access to the reservoir, except for a port on a fluid sampling system on the outside of the casing. Both wells are extensively instrumented and monitored with fibre optics as well as casing and tubing conveyed pressure and temperature monitoring systems. Other surface monitoring systems at the site include:

- an array of 630 permanently mounted geophones, used for passive seismic detection and 4D seismic imaging,
- 6 broadband seismometers for more sensitive monitoring of microseismic events related to CO_2 injection,
- a grid of water wells and soil gas sampling stations to monitor stability of surface gas composition, and

- tiltmeters and Interferometric Synthetic Aperture Radar (InSAR) reflectors to monitor surface deformations.

CO_2 at Aquistore is injected into the Cambrian Deadwood and Winnipeg formations. The Winnipeg, sitting conformably on top of the Deadwood, consists of the lowermost Black Island Sand, which is perforated in the Aquistore well. Above this is the Icebox Shale, a 30 m thick shale that for the purposes of CO_2 storage is the main sealing unit. The Deadwood is a thick and very wide-spread mixed siliciclastic unit that marks the beginning of sedimentary deposition on top of the Precambrian surface throughout much of the central Great Plains of Canada and the USA (Kreis et al., 2004). At the Aquistore site, the Deadwood is 147 m thick, and consists of interbedded sandstone, siltstone, and shale. There are four porous sandy intervals that are perforated in the injection well, with a total thickness of 150 m (Rostron et al., 2014). These zones all exhibit porosities in the 10-15 % range (White et al., 2016). For the purpose of CO_2 injection, the best zone seems to be the second interval from 3226-to 3240 meters below kelly bushing. Spinner surveys and modelling exercises suggest that this is also the zone that is taking the bulk of the injected CO_2 (Rangriz Shokri et al., 2019; Dalkhaa et al., 2019).

2. METHODOLOGY

To assess the feasibility of a CO_2 circulation test, we build a simplified, homogeneous model of the Aquistore storage site using the CMG-GEM simulation software package (Computer Modelling Group Ltd., 2020). Due to the current license limitations, our isothermal flow model is set up only for the second perforated interval of the injection site (3226-3240 m) and restricted to 10000 grid cells, **Figure 1**. The flow model employs the Peng-Robinson equation of state (Peng and Robinson, 1976) with a three-component fluid system of CO_2, methane (C1) and brine. For brevity, we refer to the produced CO_2 as gas, instead of as supercritical CO_2. This also underlines the dominant character (e.g. gas-like dynamic viscosity) of supercritical CO_2, relevant for this investigation. **Table 1** provides an overview of the main model parameters. For the calibration process of the model, employing CO_2 breakthrough and cumulative injected volumes, please see Hau (2020).

Parameter	Value
Model size	156 m x 96 m x 12 m (Figure 1)
Porosity	7.3 %
Effective permeability: - XY-direction - Z-direction	 23.8 mD 2.38 mD
Fluid components	Brine, CO_2, and CH_4 (trace comp.)
Salinity	300000 ppm
Reservoir temperature	120°C
Reservoir fluid pressure	32.5 MPa
Injection well fluid pressure at reservoir depth (Max. BHP)	42.5 MPa
Observation well fluid pressure at reservoir depth (Min. BHP)	22.5 MPa
Equation of state	Peng-Robinson (Peng and Robinson, 1976)
Initial conditions	Hydrostatic equilibrium Isothermal Fully saturated with brine

Table 1. Key model parameters of the CO_2 injection model.

In the here numerically investigated conceptual CO_2 circulation study, we assume a producer (the current observation well), located 151 m away from the injector, with a production well tubing diameter (d_{well}) of 0.11 m. Two different data sets of high and low relative permeability with respect to CO_2 flow (Bennion and Bachu, 2005; Guyant et al., 2015) are used to build the extreme base case scenarios for CO_2 injection. The well constraints for fluid injection/back-production are set to a bottomhole pressure (BHP) of 32.5 MPa ± 10 MPa. Hence, the maximum pressure difference between injector and producer is 20 MPa. By a gradual increase/decrease of BHPs at the beginning, we can create a smooth build-up of the pressure difference between the two wells. Note that the flow rate in the production well is a function of this pressure difference.

The effect of relative permeability on the performance of CO_2 circulation can be seen in **Figure 2**, which compares the CO_2 distribution from the theoretical model of **Equation 1** (Buckley and Leverett, 1942) with the numerical results of the CMG-GEM simulation. Additional information on assumptions, limiting factors, and derivation of Equation 1 can be found elsewhere (e.g. Buckley and Leverett, 1942; Hau, 2020; Ezekiel et al., 2021).

$$S_\alpha = \frac{\frac{k_{rel_\alpha}}{\mu_\alpha}}{\frac{k_{rel_\alpha}}{\mu_\alpha} + \frac{k_{rel_\beta}}{\mu_\beta}} \tag{1}$$

In Equation 1, S_α describes the saturation of phase α at a certain position and $k_{rel_{\alpha,\beta}}/\mu_{\alpha,\beta}$ is the mobility of phase α,β, with k_{rel} and μ being the relative permeability and the fluid dynamic viscosity, respectively.

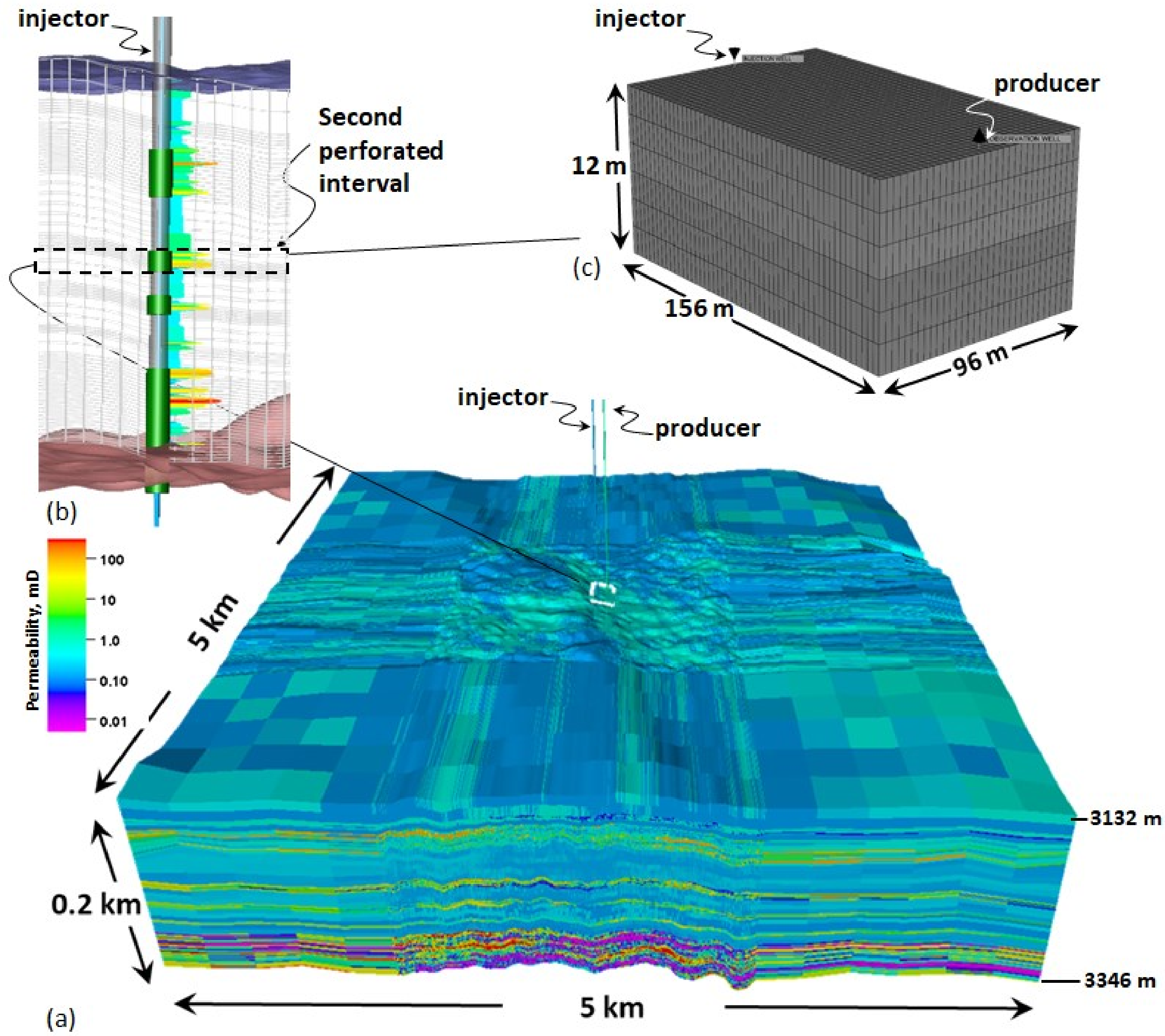

Figure 1: (a) Full geological model developed for the Aquistore geologic CO_2 storage site over a 5 km x 5 km grid monitored by permanent seismic geophones with injection and observation wells, (b) vertical cross section of the injection well, where locations of four perforated intervals are indicated with green cylinders. Also shown is the permeability distribution from well log data along the injection wellbore; warm colours represent higher permeabilities, and (c) our simplified model used here to conduct a first, conceptual simulation of a CO_2 circulation test at the Aquistore geologic CO_2 storage site.

Figure 2 shows that the relative permeability data from Guyant et al. (2015) leads to a higher well CO_2 gas saturation at a lower reservoir CO_2 gas saturation, compared to the case when employing relative permeability data from Bennion and Bachu (2005). A minimum reservoir CO_2 gas saturation exists, where the production well is almost fully saturated with CO_2 gas, as illustrated by the red line in Figure 2. Our analysis indicates that the computed CO_2 gas distribution from the theoretical model, Equation 1, (solid curve in Figure 2) is reasonably comparable to the CO_2 saturation obtained from numerical CMG-GEM simulations (dashed curve in Figure 2). We speculate that the small differences shown in Figure 2 are related to numerical issues (e.g. model dimension, limited number of grid cell, large grid cell size - all related to our currently limited CMG-GEM software license).

Adopting the approach of Ezekiel et al. (2021), we calculate a flow regime map for the production well with a well diameter of 0.11 m. This flow regime map is site-specific and is used in the next section to determine the flow regimes for the simulated scenarios for a CO_2 circulation test.

It is important to emphasise that for a successful CO_2 circulation pilot test, liquid loading in the production well must be avoided. Liquid loading describes the accumulation of a liquid phase in a multi-phase fluid production well. In general, this phenomenon occurs if the total mass flow rate and the gas saturation of the multi-phase production stream are too low. Thus, to facilitate a successful CO_2 circulation test, it is crucial to establish a constant production rate in the producer that leads to annular flow with a maximum CO_2 saturation.

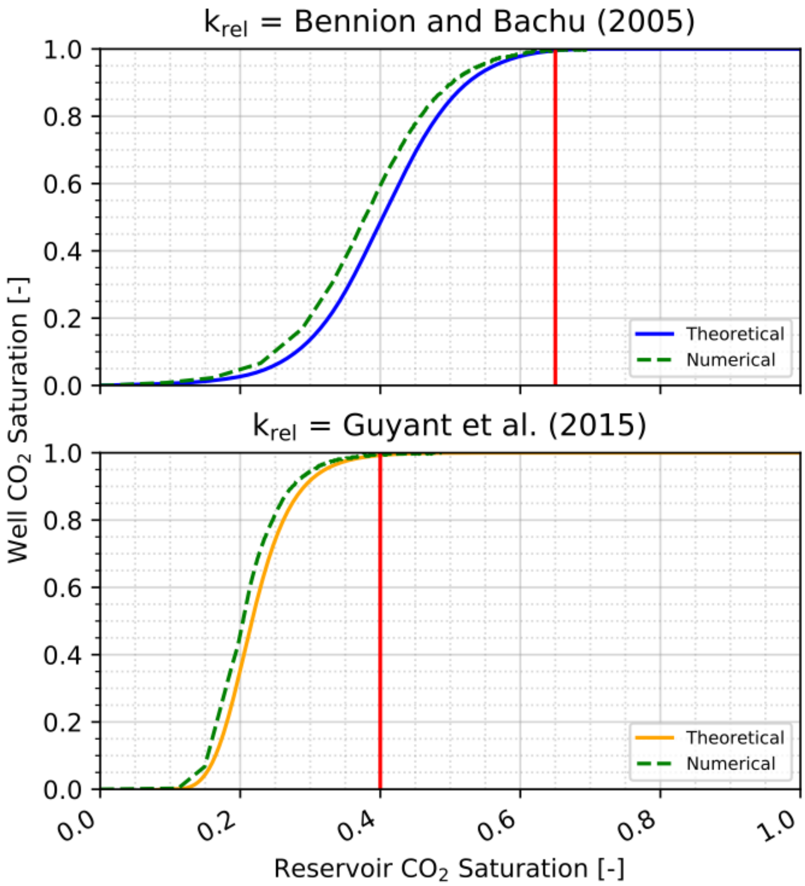

Figure 2: Base case model CO_2 gas distribution in the reservoir and the production well for both underlying relative permeability data sets. The data sets are a) measured from core plugs of the Deadwood formation, recovered at another location (Bennion and Bachu, 2005) and b) modelled with the van-Genuchten-Mualem model (Guyant et al., 2015). As described in the main text, the solid curves compare the analytically obtained CO_2 gas distribution (see Equation 1) with the dashed curves, representing the numerically obtained CO_2 gas distribution. Moreover, the red lines indicate the reservoir CO_2 gas saturation that leads to an almost fully CO_2-saturated production well. The figure was modified from Hau (2020).

3. SIMULATION RESULTS

Figure 3 through **Figure 5** follow the same structure. The upper diagram always displays the simulation data obtained with the relative permeability data set from Bennion and Bachu (2005), while the lower diagram shows the data obtained from the relative permeability data set proposed by (Guyant et al., 2015). Each figure follows identical colour coding. Simulation results obtained from a numerical model with an underlying absolute permeability of k_{abs} = 23.8 mD are shown in orange. The other colours (red, blue, and green) indicate underlying absolute model permeabilities of k_{abs} = 100 mD, 200 mD, and 300 mD, respectively.

Figure 3 summarises the daily fluid production rates for all eight modelled, nine-months-long CO_2 circulation simulations (see Section 2). The daily fluid production rates are given at reservoir conditions. In the figure, the continuous lines correspond to the daily total fluid production rate. Additionally, the dashed and dotted lines indicate the daily CO_2 gas and liquid brine production rates, respectively. The smooth increase of the production rates, visible during the first 14 to 21 days of fluid production, is due to predefined well constraints.

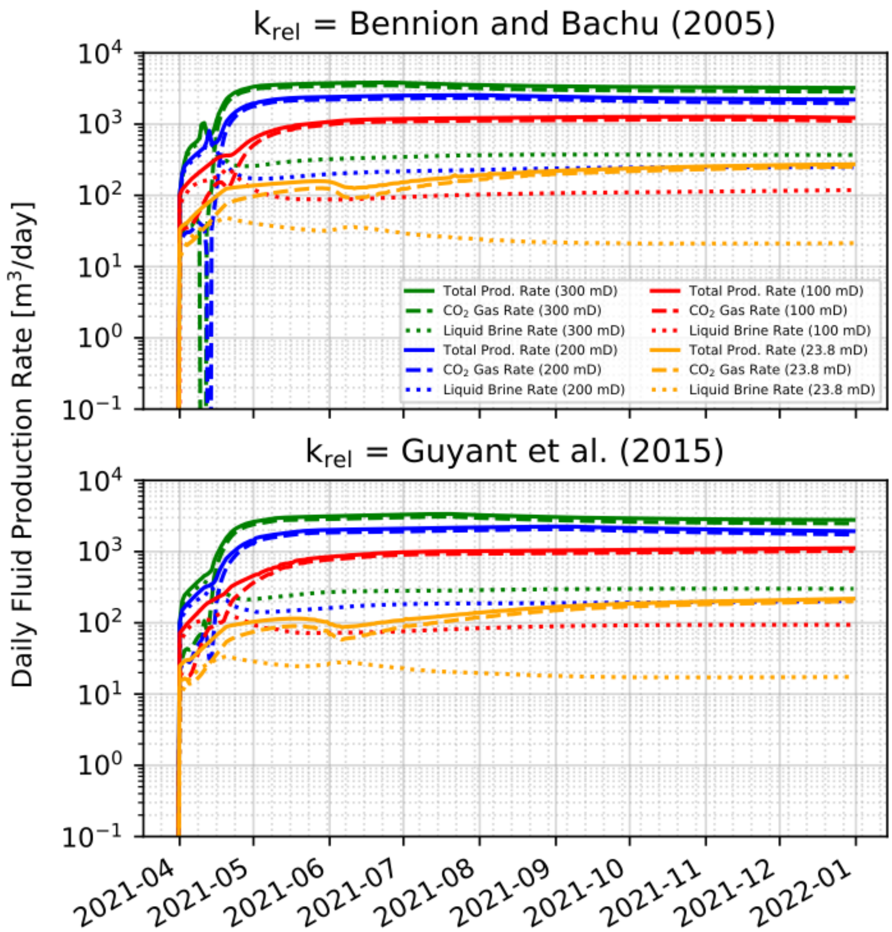

Figure 3: Daily fluid flow rates (in m^3/day) in the production well for multiple assumed absolute permeabilities (in mD) and two different underlying relative permeability data sets (top versus bottom panel) as described in the main text. Note that the daily fluid production rate axis is logarithmic. The figure was modified from Hau (2020).

In general, Figure 3 illustrates that constant production rates will be reached within weeks to a few months after fluid production started. Importantly, at constant production fluid flow rates, the produced fluid is dominated by CO_2 gas. The volume of daily produced CO_2 gas is up to one order of magnitude larger than that of liquid brine (note that the daily fluid production rate axis is logarithmic in Figure 3). However, during the stabilisation period, immediately after commencing fluid production, predominantly liquid brine is produced. Before constant flow rates are reached, a second, typically small, drop in the daily fluid production rate can be observed. The time required to reach constant flow rates is inversely proportional to the formation's modelled absolute permeability (higher k_{abs} values result in shorter durations). Finally, higher absolute permeabilities generate higher fluid production rates.

Figure 4 shows the CO_2 gas (versus liquid brine) saturation fraction in the reservoir pore space (dashed lines) and in the production well (solid lines). The former is obtained from the reservoir grid cell surrounding the assumed production well inlet. All simulations eventually lead to a constant CO_2 gas saturation fraction of 85% to 90% in the production well (solid lines), independent of the relative permeability data assumed (top versus bottom panel). In contrast, the constant reservoir pore space CO_2 gas saturation fractions (dashed lines) depend on the underlying relative reservoir permeability data (top versus bottom panel). For instance, the numerical model, based on the relative permeability data from Bennion and Bachu (2005), ultimately reaches a constant CO_2 gas saturation fraction in the reservoir pore space of around 50%. In contrast, the model, based on the relative permeability data from Guyant et al. (2015) results in a much lower reservoir pore space CO_2 gas saturation of approximately 30%.

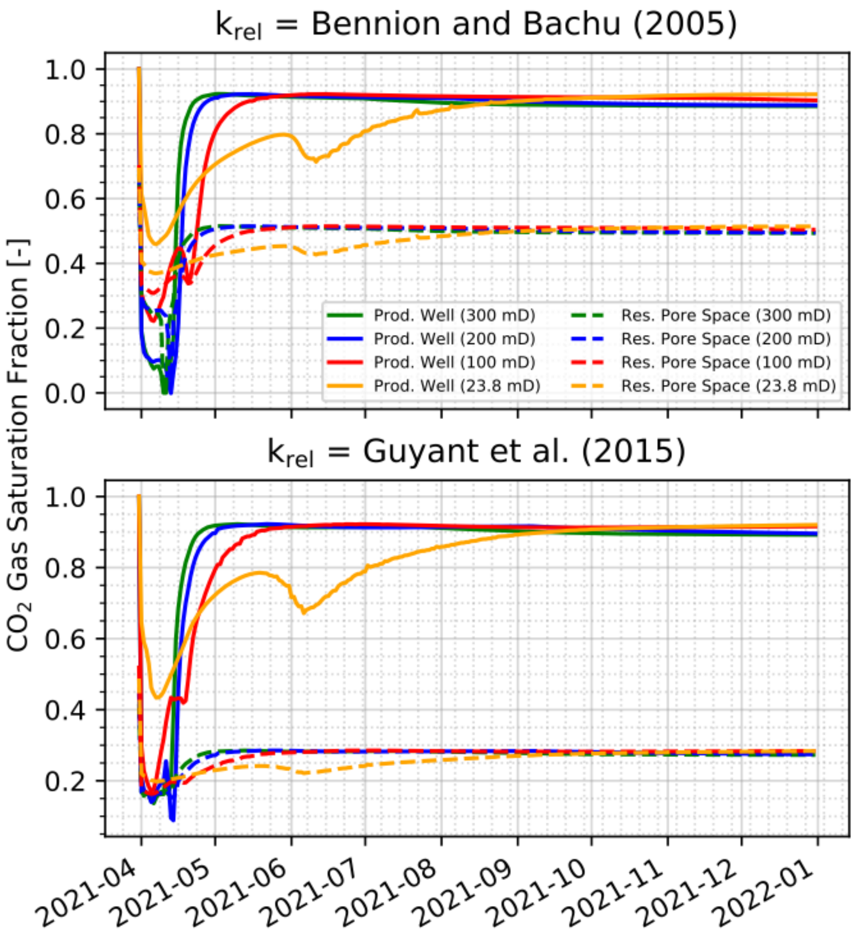

Figure 4: Diagrams showing the CO_2 gas (versus liquid brine) saturation fraction in the reservoir pore space (dashed lines) and the production well (solid lines), depending on the underlying relative permeability data (top versus bottom panel) and absolute reservoir permeabilities (in mD) assumed. The figure was modified from Hau (2020).

Immediately after commencing fluid production, all modelled scenarios show a drastic drop of the CO_2 gas saturation fraction. Depending on the underlying absolute and relative permeabilities, this drop is more or less pronounced. Moreover, the CO_2 gas saturation fraction drop is less distinct in the reservoir pore space than in the production well. Evidently, increasing the reservoir's absolute permeabilities causes more pronounced CO_2 gas saturation fraction drops. Further, higher absolute permeabilities lead to faster CO_2 gas saturation recoveries. Besides the initial saturation drop, a second CO_2 gas saturation fraction drop is visible in both diagrams. With decreasing absolute permeabilities, the duration between both saturation drops increases. Finally, numerical instabilities are noticeable, i.e. winding/jumping of the continuous blue, red, and orange lines.

Figure 5 shows the daily total fluid mass flow rate superimposed onto the previously calculated, site-specific well flow regime map (see Section 2). The total fluid mass flow rate is given at reservoir conditions on a logarithmic y-axis. Each data point represents one day of the nine-months-long simulation. The start of fluid production is indicated by t_0 and the end of simulation is given by t_{end}. Consistent with Figures 3 and 4, Figure 5 shows a drop in the CO_2 mass fraction immediately after fluid production commences. Despite this drop in CO_2 mass fraction, the total mass flow rate increases continuously, indicating high and increasing brine production rates. Figure 5 also shows the second CO_2 gas saturation drop. The time until constant mass flow rates are reached varies and depends on the underlying absolute reservoir permeability used. The highest assumed absolute permeability, $k_{abs} = 300$ mD, reaches steady-state conditions within less than a month. In contrast, the scenario with the smallest absolute permeability, $k_{abs} = 23.8$ mD, requires multiple months to reach stable fluid mass flow rates. Annular flow, with constant flow rates in the production well, is reached if the underlying absolute reservoir permeability is at least 100 mD. As described in Section 2, the total fluid mass flow rate, shown in Figure 5, represents the maximum flow rate possible that can be achieved with a pressure differential between the injector and the producer of 20 MPa.

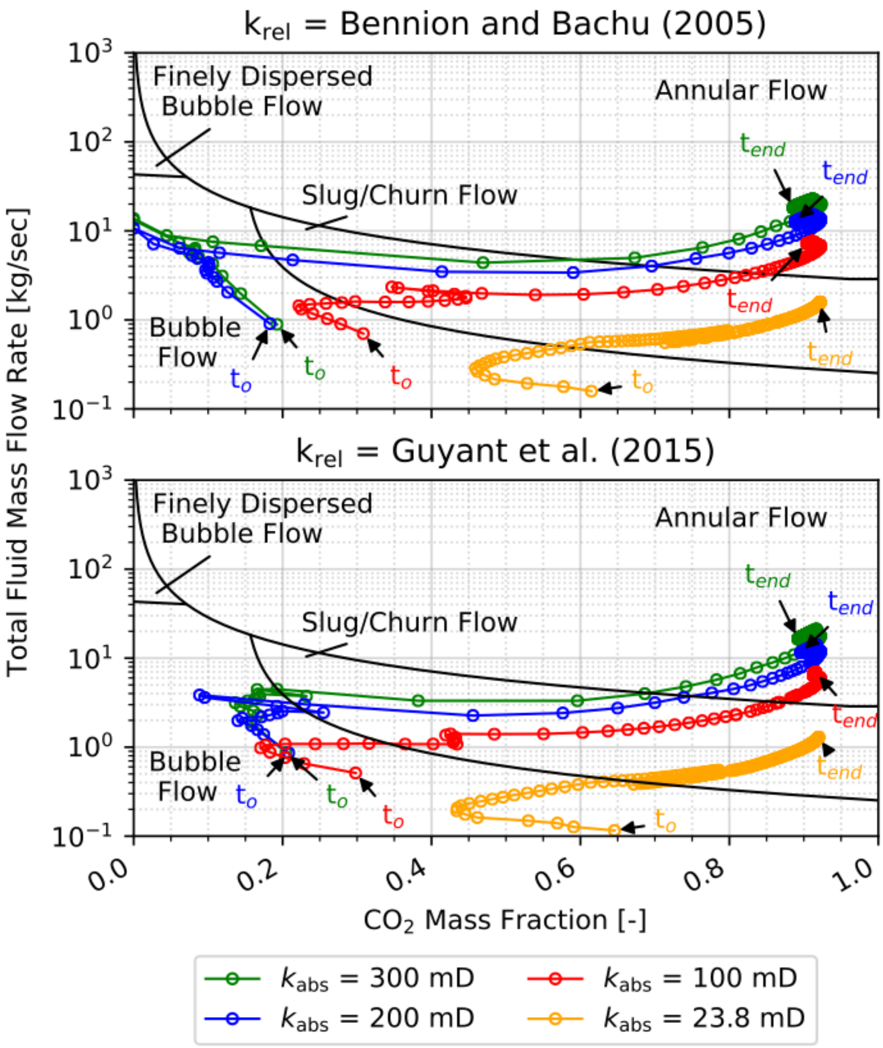

Figure 5: Obtained total produced fluid mass flow rates for all modelled scenarios, superimposed onto an analytically determined fluid flow regime map for a production well with a diameter of d_{well} = 0.11 m. Each data point represents one day of the nine-months-long simulation. t_0 and t_{end} indicate the start and the end of the simulations, respectively. k_{abs} stands for the underlying absolute reservoir permeability of the model. The top versus the bottom panel represent different relative reservoir permeabilities used. The figure was modified from Hau (2020).

4. DISCUSSION

The presented work is a first-order, conceptual numerical study to examine the responses of CO_2 circulation at the Aquistore CCS site in southern Saskatchewan, Canada. Our simplified homogeneous numerical model assumes isothermal conditions and is currently not meant to rigorously match the CO_2 injection history. Inclusion of a non-isothermal CO_2 injection history should be addressed in future models as the intermittent cold CO_2 injection has resulted in episodic transient heat and fluid flow conditions within the Aquistore storage formations (Rangriz Shokri et al., 2019), likely affecting the outcome of a CO_2 circulation test.

Our numerical analysis indicates that the fluid production rates are scaled mainly by the absolute permeability of the reservoir. This is important because the Aquistore injection well was perforated at four different intervals with inter-bedded shales (Talman et al., 2020). The vertical and horizontal heterogeneities of petrophysical properties of each interval can alter the multiphase fluid pathways and flow rates from the injector to the producer. This affects the CO_2 gas (versus liquid brine) saturations within the CO_2 plume. Our simulation results suggest that a 12 m thick reservoir, with an assumed absolute permeability of 100 mD or more, will eventually lead to constant fluid flow rates and an annular flow regime in the production well (Figure 5). Immediately after commencing fluid production, the CO_2/brine mass ratio is very small (low CO_2 gas flow rates and high liquid brine flow rates), however, once steady-state conditions are reached within weeks to a few months, the CO_2/brine ratio increases so that mainly CO_2 gas is produced (Figure 3).

In all our modelled scenarios, the initiation of CO_2 circulation is followed by an immediate CO_2 gas saturation fraction drop in the production well. We speculate that the drying-out process of the pore space surrounding the assumed production well inlet leads to such a CO_2 saturation drop. In line with this observation, Figure 4 suggests that lower absolute permeabilities in the CO_2 storage formation can result in smaller, but longer-lasting, CO_2 saturation drops. In contrast, higher absolute permeabilities lead to sharp CO_2 saturation drops, but they more quickly reach a constant, steady-state CO_2 saturation. Such observations highlight the importance of detailed reservoir characterisations and determinations of CO_2 saturations in the vicinity of (planned) injection and production wells when planning CPG operations. At Aquistore, pulsed neutron density (PND) measurements are continuously conducted to monitor temporal fluid saturation changes close to the observation well (Kennedy, 2017). We highly recommend that the knowledge of CO_2 saturation (e.g. from PND logs and seismic surveys) is included prior to any CO_2 circulation pilot test and later CPG operations.

Another key factor that might affect the performance of a CO_2 circulation test is relative permeability. Comparing Figure 2 with Figure 4, we observe that higher relative permeabilities to CO_2 result in a lower residual CO_2 saturation in the pore space. This relationship is important to understand because higher residual CO_2 saturations require higher CO_2 volumes to be present in the reservoir pore space before the production well can reach a, for annular flow, required CO_2 saturation fraction. Also, Figure 4 shows that, once the residual CO_2 gas saturation is reached, CO_2 preferably flows into the well, rather than remaining in the reservoir. Thus, in cases where only a limited amount of CO_2 is available, it is favourable to target horizons with higher relative permeabilities, especially for multi-horizon CO_2 storage sites, such as Aquistore. After all, such horizons are also the ones with the highest absolute permeabilities.

Our simulations further suggest that the minimum time required to “dry-out” the reservoir (i.e. having replaced most of the liquid brine with CO_2 gas) is weeks to a few months, for the here-modelled scenarios. This duration is the time required until steady-state conditions, with constant fluid flow rates, are established during the CO_2 circulation test. As stated earlier, the dry-out times seem to positively correlate with the absolute permeability of the storage formation. This highlights the significance of issues such as near-wellbore permeability enhancement due to induced-thermal fracturing, changes in relative permeabilities, hysteresis, enhanced imbibition zones, and salt precipitation (i.e. reduction in permeability) around the injection/production wells.

In addition to the properties of geological CO_2 storage formations, the flow patterns of CO_2 gas and liquid brine in the wellbore are also of utmost importance. In this study, we use the Turner flow criterion (Taitel et al., 1980; Ezekiel et al., 2021), which was originally developed and calibrated for oil and natural gas wells. A look at previous studies suggests that the traditional Turner criterion overestimates the velocity required to reach the annular flow regime (Liebscher et al., 2017). Thus, during a CO_2 circulation test, annular flow would probably be established at lower production fluid flow velocities than expected from the Turner criterion. With respect to our feasibility study here, this velocity overestimation assures that our flow regime estimations are conservative, meaning that annular fluid flow in the production will (critical to avoid liquid loading) is more easily achieved than modelled here, given the here-modelled scenarios. However, an updated Turner criterion for (supercritical) CO_2 production will be considered in future studies.

5 CONCLUDING REMARKS

Our analysis suggests that stable CO_2 circulation can be achieved at the Aquistore CO_2 storage site. In the majority of our simulated scenarios, employing different absolute and relative permeability assumptions, we observe that constant total mass flow rates, with high CO_2 saturations, would lead to annular flow in the production well, thereby avoiding liquid loading in the production well. The “dry-out” time was found to positively correlate with the absolute permeability of the CO_2 storage formation, lasting from weeks to a few months under the here-modelled scenarios for the Aquistore CCS site.

Our model is restricted to the second perforated interval of the Aquistore CO_2 injection well only, due to CMG-GEM software license limitations. We thus recommend follow-up studies to address the uncertainties associated with reservoir characterisation and model set-up prior to any CO_2 circulation and/or CPG pilot test. These studies should include investigating issues such as petrophysical reservoir heterogeneities, production from multiple perforated zones, presence of a regional leaking aquifer, design of well completions and optimisation of injection/production constraints, among others. The model should also be more rigorously history-matched to the CO_2 injection history at Aquistore.

6 ACKNOWLEDGEMENTS

The first author would like to thank the IDEA League for the opportunity to write his MSc thesis under the supervision of M.O. Saar at ETH Zurich, Switzerland, as part of the Joint MSc Masters Programme in Applied Geophysics. The work presented here is mostly based on that MSc thesis. We also thank the Werner Siemens Foundation (Werner Siemens-Stiftung) for its support of the Geothermal Energy and Geofluids (GEG.ethz.ch) group at ETH Zurich. We further gratefully acknowledge the Petroleum Technology Research Centre (PTRC), Regina, Saskatchewan, Canada, for discussions and advice regarding the Aquistore geologic CO_2 storage site, which they operate. The second (ARS) and fourth (RJC) authors gratefully acknowledge the Swiss Federal Office of Energy and the Energi Simulation Industrial Research Chair in Reservoir Geomechanics in Unconventional Resources.

REFERENCES

Adams, B. M., T. H. Kuehn, J. M. Bielicki, J. B. Randolph, and M. O. Saar (2015). “A comparison of electric power output of CO2 Plume Geothermal (CPG) and brine geothermal systems for varying reservoir conditions”. In: Applied Energy 140, pp. 365–377. doi: 10.1016/j.apenergy.2014.11.043.

Adams, B. M., D. Vogler, T. H. Kuehn, J. M. Bielicki, N. Garapati, and M. O. Saar (2020). “Heat depletion in sedimentary basins and its effect on the design and electric power output of CO2 Plume Geothermal (CPG) systems”. In: Renewable Energy. doi: 10.1016/j.renene.2020.11.145.

Bennion, B. and S. Bachu (2005). “Relative Permeability Characteristics for Supercritical CO2 Displacing Water in a Variety of Potential Sequestration Zones”. In: SPE Annual Technical Conference and Exhibition. Society of Petroleum Engineers. doi: 10.2118/ 95547-ms.

Buckley, S. E. and M. C. Leverett (1942). “Mechanism of Fluid Displacement in Sands”. In: Transactions of the AIME 146, pp. 107–116. doi: 10.2118/942107-g.

Computer Modelling Group Ltd. (2020). Software documentation (2019 General Release).

Dalkhaa, C. et al. (2019). "An Improved Numerical Modeling and Simulation Study of the Aquistore CO2 Storage Project". In: SSRN Electronic Journal. doi: 10.2139/ ssrn.3365731.

Ezekiel, J., B. M. Adams, M. O. Saar, and A. Ebigbo (2021). "Numerical analysis and optimization of the performance of CO2-Plume Geothermal (CPG) production wells and implications for electric power generation". In: Geothermics (Under Review).

Garapati, N., J. Randolph, and M. Saar (2015). "Brine displacement by CO2, energy extraction rates, and lifespan of a CO2-limited CO2-Plume Geothermal (CPG) system with a horizontal production well". In: Geothermics 55, pp. 182–194. doi: 10.1016/ j.geothermics.2015.02.005.

Global CCS Institute (2020). Global Status of CCS 2020. Tech. rep. The Global CCS Institute.

Guyant, E., W. S. Han, K. .-Y. Kim, M. .-H. Park, and B. .-Y. Kim (2015). "Salt precipitation and CO2/brine flow distribution under different injection well comple- tions". In: International Journal of Greenhouse Gas Control 37, pp. 299–310. doi: 10.1016/j.ijggc.2015.03.020.

Hau, K. P. (2020). "Feasibility of a CO2 Plume Geothermal (CPG) Pilot at the Aquistore (Canada) CCS site". MA thesis. ETH Zürich.

Kennedy, M. (2017). Interpreting CO2 Saturation Changes from Pulsed Neutron Logs at the Aquistore Site. Report for the Petroleum Technology Research Centre.

Kreis, L., K. Ashton, and R. Maxeiner (2004). "Geology of the Precambrian basement and Phanerozoic strata in Saskatchewan; Lower Paleozoic Map Series-Saskatchewan; Sask". In: Industry Resources, Misc. Rep 8.

Liebscher, A., B. Wiese, F. Möller, and A. Bannach (2017). "Understanding Well Load-up Behaviour in CO2 Wells During CO2 Back-production Field Test at the Ketzin Pilot Site, Germany – Turner Criterion Revisited". In: Energy Procedia 114, pp. 4188–4192. doi: 10.1016/j.egypro.2017.03.1559.

Peng, D.-Y. and D. B. Robinson (1976). "A New Two-Constant Equation of State". In: Industrial & Engineering Chemistry Fundamentals 15.1, pp. 59–64. doi: 10.1021/ i160057a011.

Randolph, J. B. and M. O. Saar (2011a). "Combining geothermal energy capture with geologic carbon dioxide sequestration". In: Geophysical Research Letters 38, n/a–n/a. doi: 10.1029/2011gl047265.

Randolph, J. B. and M. O. Saar (2011b). "Coupling carbon dioxide sequestration with geothermal energy capture in naturally permeable, porous geologic formations: Implications for CO2 sequestration". In: Energy Procedia 4, pp. 2206–2213. doi: 10.1016/j.egypro.2011.02.108.

Rangriz Shokri, A., R. J. Chalaturnyk, and E. Nickel (2019). "Non-Isothermal Injec- tivity Considerations for Effective Geological Storage of CO2 at the Aquistore Site, Saskatchewan, Canada". In: SPE Annual Technical Conference and Exhibition. Society of Petroleum Engineers. doi: 10.2118/196118-ms.

Rostron, B., D. White, C. Hawkes, and R. Chalaturnyk (2014). "Characterization of the Aquistore CO2 project storage site, Saskatchewan, Canada". In: Energy Procedia 63, pp. 2977–2984. doi: 10.1016/j.egypro.2014.11.320.

Taitel, Y., D. Bornea, and A. E. Dukler (1980). "Modelling flow pattern transitions for steady upward gas-liquid flow in vertical tubes". In: AIChE Journal 26.3, pp. 345–354. doi: 10.1002/aic.690260304.

Talman, S., A. Rangriz Shokri, R. Chalaturnyk, and E. Nickel (2020). Salt Precipitation at an Active CO 2 Injection Site. doi: 10.1002/9781119593324.ch11.

White, D. J., C. D. Hawkes, and B. J. Rostron (2016). "Geological characterization of the Aquistore CO2 storage site from 3D seismic data". In: International Journal of Greenhouse Gas Control 54, pp. 330–344. doi: 10.1016/j.ijggc.2016.10.001.